Solar Energy Materials & Solar Cells 94 (2010) 465–470

Contents lists available at ScienceDirect

Solar Energy Materials & Solar Cells

journal homepage: www.elsevier.com/locate/solmat

Thickness dependence and solution-degradation effect in poly (3-hexylthiophene):phenyl-C61-butyric acid methyl ester based solar cells

Hui Jin*, Juuso Olkkonen, Markus Tuomikoski, Pälvi Kopola, Arto Maaninen, Jukka Hast

VTT Technical Research Centre of Finland, P. O. Box 1100, FI-90571 Oulu, Finland

ARTICLE INFO

Article history:
Received 26 August 2009
Received in revised form
4 November 2009
Accepted 5 November 2009
Available online 1 December 2009

Keywords:
Photovoltaic
Polymer
Fullerene
Film thickness
Degradation

ABSTRACT

The performance of bulk-heterojunction solar cells made with poly(3-hexylthiophene) (P3HT) as the donor and phenyl-C61-butyric acid methyl ester (PCBM) as the acceptor depends strongly on various factors in fabrication processes. This work studies the effect of the thickness of the P3HT:PCBM layer produced in the spin coating process on photovoltaic performances. Thickness dependent optical absorption in P3HT:PCBM layer is numerically modelled and the results are compared with experimental data. In addition, it is analyzed how degradation of air-exposed P3HT:PCBM blends depends on the storage time in nitrogen atmosphere.

1. Introduction

As a potential alternative for low-cost renewable energy sources, polymer-based solar cells have been widely studied and rapidly developed in recent years. Poly (3-hexylthiophene) (P3HT) and phenyl-C61-butyric acid methyl ester (PCBM) have become promising materials exhibiting power conversion efficiency about 4% [1,2]. On the road to improve the efficiency of polymer-based solar cells, various attempts have been taken in the fabrication processes, such as thermal annealing, solvent annealing, post-treatment and so on. In fact, processing in the fabrication plays an extremely important role for improving the performance of plastic solar cells.[3,4]

The thickness of P3HT:PCBM film is related to the absorption efficiency and the charge transport of solar cells, and the optimal thickness of P3HT:PCBM film has been reported to be around 210–230 nm [5]. However, research groups have used various thicknesses between 80 and 220 nm to obtain the similar efficiencies [6–8]. In this work, the thickness dependent optical absorption in P3HT:PCBM layer was modelled. It was found that the modelled data agreed well with the experimental results.

The degradation of P3HT:PCBM samples have been investigated by several research groups [9–13]. However, the degradation mechanism of the photoactive solutions and its effect on the resulting solar cells is still ambiguous and worth further study, since it would be closely involved with the development of printing ink, the fabrication of organic photovoltaic modules and even the roll-to-roll manufacture of flexible polymer solar cells [14–17]. In this work, the effect of air exposure of blends on the fabricated solar cells was analyzed via current–voltage characteristics, optical absorption spectra and Raman spectroscopy.

2. Experimental details

The indium tin oxide (ITO)-coated glass substrates were cleaned by ultrasonic treatment in deionized water, acetone and isopropyl alcohol sequentially, followed by N2-gas blowing to dry. After the UV–ozone treatment for 3 min, the square resistance of ITO-coated glass can be 16–17 Ω/κ. The solution of poly(3,4-ethylenedioxythiophene): poly(styrenesulphonate) (PEDOT:PSS) (Clevios P VP Al 4083) was filtered by 0.45 μm PVDF filter and then spin-coated on the UV–ozone treated ITO glass. The resulting PEDOT:PSS film was heated on a hot plate at 150 °C for 20 min and the thickness was about 35–40 nm, measured by Veeco Dektak 150. P3HT and PCBM were directly used to be blended as purchased from Rieke Metals and Nano-C. The P3HT:PCBM weight ratio was about 1:1 (if no special explanation). The solutions were prepared by dissolving solid materials into dried 1,2-dichlorobenzene (DCB) in a glove box. Immediately after the solution passed through 0.45 μm Acrodisc filter, the photoactive layers were spin-coated on PEDOT:PSS film in the air. When the colour of photoactive layers turned to dark purple, the samples were transferred to the glove box for performing a thermal annealing process and then put in the

* Corresponding author. Tel.: +358 40 4865373, fax: +358 20 722 2320.
E-mail address: hui.jin@vtt.fi (H. Jin).

0927-0248/$ - see front matter © 2009 Elsevier B.V. All rights reserved.
doi:10.1016/j.solmat.2009.11.007

evaporator to deposit metal top electrodes. If there is no special explanation, thermal annealing was processed at 110 °C for 5 min and the cathode consisted of Ca (25 nm) and Ag (80 nm). The shadow mask of ~10 mm^2 utilized during cathode deposition defined the active area of the device. All devices were encapsulated by UV-cured epoxy (DELO 681) in the glove box with dry nitrogen atmosphere.

The thickness of photoactive layer was controlled by setting the spin speed and the concentration of the solution. The P3HT master solutions are 17, 20, 22 and 25 mg/ml in DCB. PCBM was dissolved in the P3HT master solutions with the ratio of about 1:0.95 (P3HT:PCBM). Fig. 1 shows the thickness of the P3HT:PCBM films as a function of the spin speed for four concentrations. The spin speeds of 600, 800, 1000 and 1200 rmp were selected because a speed lower than 600 rmp easily caused a non-uniform film and a speed higher than 1200 rmp easily led to a bad morphology due to the fast solvent evaporation before the thermodynamic balance was achieved. By using these selected concentrations and spin speeds, two batches of samples with 15 thicknesses were prepared. For each thickness, 4–6 samples were tested for the average and the error value. The first batch was prepared by using the master solution of 17 and 20 mg/ml, and tested under the illumination of 100 mW/cm^2, while the second batch was prepared by using the solution of 22 and 25 mg/ml, and tested under the illumination of 85 mW/cm^2. The cathodes for all the samples in the two batches were Ca-20 nm/Al-100 nm.

Three batches of blend solutions (1#, 2# and 3#) were prepared for studying the degradation of the solutions after exposed to air for a few hours and stored in a glove box for a time. The solutions were prepared in the glove box by dissolving PCBM into 20 mg/ml P3HT DCB solutions. The ratios of P3HT:PCBM were about 1:1. After the blend solutions were ready, a fresh sample was prepared immediately for comparison. The remaining solutions were stored for preparing studied samples. Solutions 1#, 2# and 3# were stored in the glove box for 5, 12 and 55 days after exposed to air for a few hours, and a part of solution 2# was directly stored for 12 days and never exposed to air.

The characterization was done on the encapsulated samples in the ambient air at room temperature. Current–voltage curves were recorded with a Keithley 2400 source measurement unit. Illumination tests were carried out under AM1.5 irradiation by using a 300 W Cermax lamp-based solar simulator. The illumination setup was calibrated and proved that the irradiation of the test plane was well above the 100 mW/cm^2 specified in the IEC 904-3 standard. Ultraviolet–visible (UV–vis) absorption spectra were recorded on Varian Cary 5000 spectrophotometer. Raman spectra were collected with a scanning Raman microscope with a laser wavelength of 785 nm as the excitation source. A Peltier-cooled CCD detector (Andor Newton DU-971N-BV) with 1600 × 400 pixels was operated at −60 °C. The integration time was 1 ms and the spectral rate was 600 spectra/s.

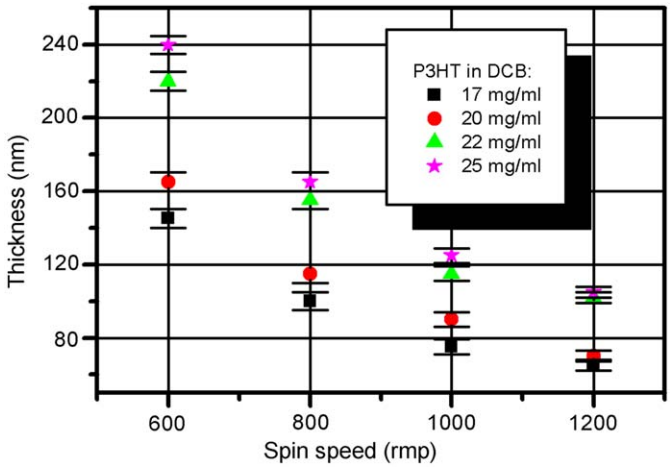

Fig. 1. The corresponding relation of the thickness of P3HT:PCBM films and the spin speed at various concentrations of solutions (P3HT: 17, 20, 22 and 25 mg/ml).

3. Results and discussion

The thickness of the photoactive layer has always been considered to have an effect on photovoltaic (PV) parameters. According to the transfer matrix formalism (TMF) [18,19], light absorption in a solar cell with the structure of Glass/ITO/P3HT:PCBM (1:1)/Ag was modelled. The refractive index of Schott BK7 was used for the glass slide and the refractive indexes of ITO, PEDOT:PSS, P3HT:PCBM, Ca and Ag were taken from the Refs. [20–24], respectively. The layer thicknesses given in Fig. 2c were chosen to correspond with the fabricated cells. TMF assumes that the incident light is perfectly monochromatic, and thus if the glass slide is included in the model, additional interference effects are seen in the results that do not coincide with the experimental data. This is due to the fact that the coherence length of visible sunlight is on the order of 1 μm [25]. Therefore, we assumed in TMF calculations that light is incident in glass and calculated the light transmittance through the first air/glass interface separately.

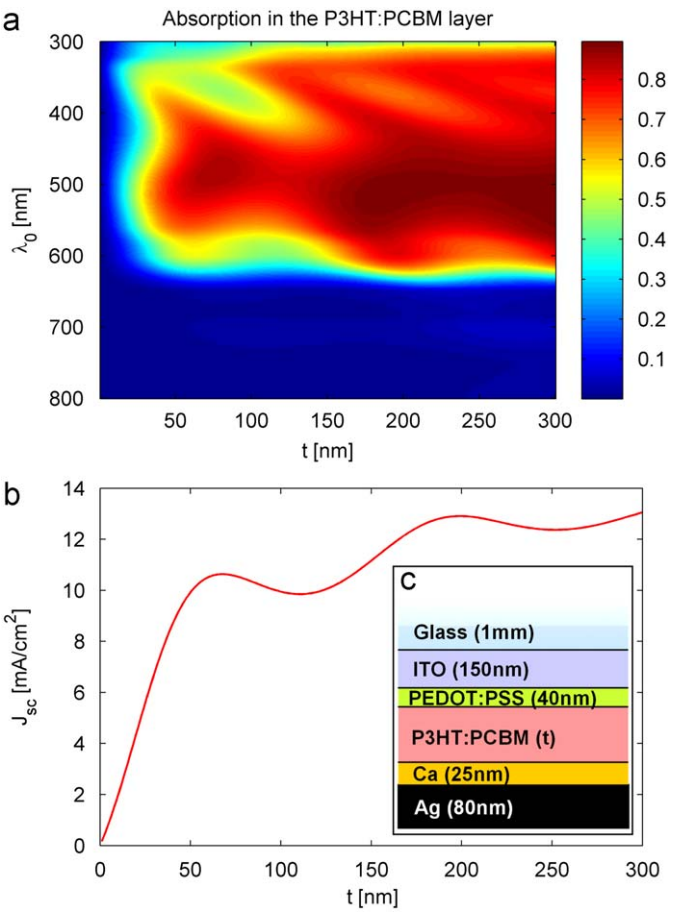

Fig. 2. (a) Simulated absorption in the P3HT:PCBM layer as a function of the photoactive layer thickness (t) and the free space wavelength of the incident light (λ_0). (b) Thickness-dependent short-circuit current of the cell (calculated from the P3HT:PCBM absorption data with the assumption of internal quantum efficiency of unity). (c) Layer thicknesses of the modelled cell.

Also, light absorption in 1 mm thick glass slide at UV wavelengths was included into the model. Fig. 2a shows the modelled absorption in the P3HT:PCBM layer as a function of the thickness of the active layer (t) and the free space wavelength of the normally incident light (λ_0). The narrow bar on the left of figures indicates the absorption density. We used this absorption data to calculate the theoretical short-circuit current (J_{sc}) with the assumption that the cell's internal quantum efficiency is unity. The absorption data was multiplied by the AM1.5G spectral irradiance and then divided by the wavelength dependent photon energy and finally integrated over the wavelength range of interest to obtain the total number of generated electron–hole pairs. The resulting P3HT:PCBM thickness dependent J_{sc} is shown in Fig. 2b. The results clearly showed that the J_{sc} exhibit two local maximums around 70 and 200 nm and local minimums around 115 nm and 250 nm. According to the following experimental results, it was found that the changes in the J_{sc} and the power conversion efficiency (η) as a function of the P3HT:PCBM film thickness were almost identical with the simulated J_{sc}.

Fig. 3 presents the PV parameters of 71 pieces of P3HT:PCBM solar cells as a function of the thickness of the P3HT:PCBM photoactive layer. The four concentrations of the solutions in the two batches produced 15 thicknesses, and the illumination intensities for the first and the second batches were 100 and 85 mW/cm^2, respectively. As can be seen, the dependence of η on the P3HT:PCBM thickness was almost identical with the modelled result shown in Fig. 2. Two local η maximums occurred at 60–80 nm and 160–220 nm, and η minimum was at 100–120 nm. The inset in Fig. 3 shows the current density–voltage (J–V) characteristics of a few typical samples with the P3HT:PCBM thickness of 165 nm and 220 nm. The best device exhibits the performances with J_{sc}=8.44 mA/cm^2, FF=0.68, V_{oc}=0.57 V and the corresponding η was 3.28% under the illumination intensity of 100 mW/cm^2. Actually, according to Fig. 3, the changes in η were mainly resulted from the changes in Jsc, since the two curves are quite similar. It indicated that the J_{sc} was the parameter that was affected most directly and significantly by the photoactive layer thickness (the lower J_{sc} for the samples with the thicker film (red solid circle in Fig. 3) was resulted from the lower illumination intensity). This conclusion is consistent with the report of Hoppe et al. [26] on the relation of photocurrent and the absorption layer thickness in polymer solar cells. The similar dependence did not occur in FF and V_{oc}, and the increased thickness of the photoactive layer caused a gradual decline in both the parameters. The changes in V_{oc} were more attributed to the decreased shunt resistance (R_{sh}), and the changes in FF should be caused by both the increased serial resistance (R_s) and the decreased R_{sh} (Table 1). The R_s and the R_{sh} can be estimated from the slope close to 1 and 0 V in term of the J–V characteristics in the dark, respectively [27]. As shown in Table 1, the increased thickness led to the increase in the average R_s and the decrease in the average R_{sh}. Since R_s and R_{sh} can be influenced by various factors except the thickness of the photoactive layer, a wide thickness range for the average values was selected for estimation, and still it can be seen that the deviation was large. As a result, although the thickness of 70–80 nm of the P3HT:PCBM film can obtain a higher efficiency due to a relative higher FF and V_{oc}, the absorption is not enough. An effective approach for a photoactive layer with thin thickness is to add an optical spacer between the photoactive layer and the metal cathode [28]. However, for P3HT:PCBM composite devices without an optical spacer, the thickness between 160 and 220 nm is recommended for sufficient absorption and charge collection, and thus higher resulting efficiency.

Fig. 4 shows how storage time affects on J–V characteristics of the devices prepared from the air-exposed solutions, using the devices fabricated from the fresh solutions as a reference. In addition, a result for 12 days stored solution never exposed to air is included in Fig. 4b. The 5-day (solution 1#), 12-day (solution 2#) and 55-day (solution 3#) storage caused a decline in η by 1%, 6.6% and 21.5%, respectively. However, the 12-day stored non-exposed solution experienced no degradation at all. Conclusively,

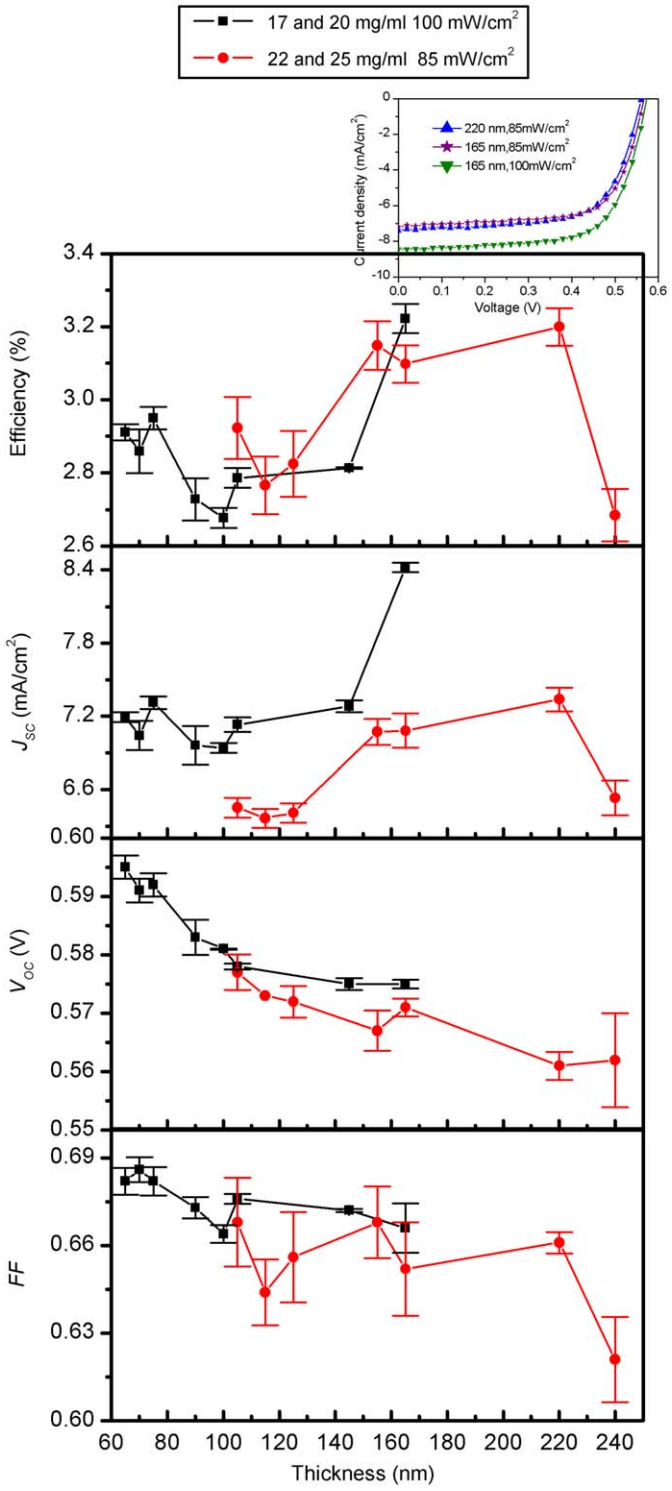

Fig. 3. The dependence of PV parameters of P3HT:PCBM solar cells on the thickness of the P3HT:PCBM photoactive layer, including batch 1 (17 and 20 mg/ml) under the illumination of 100 mW/cm^2 (square) and batch 2 (22 and 25 mg/ml) under the illumination of 85 mW/cm^2 (circle). The inset shows the typical J–V characteristics of the samples with the thickness of 165 nm or 220 nm.

Table 1
The average and deviation values of R_s and R_{sh} in the devices with the different thicknesses of the photoactive layer.

		60–80 nm	100–125 nm	145–200 nm
R_s (Ω cm^2)	Avg.	2.83	2.88	3.43
	Std.	±0.44	±0.81	±1.08
R_{sh} (MΩ cm^2)	Avg.	5.14	4.08	2.47
	Std.	±1.00	±0.60	±0.61

The cathode for the devices consisted of Ca (20 nm) and Al (100 nm).

the degradation in PV performance was gradually enhanced with the increased storage time for the air-exposed blend solution, even though the exposure time was just a few hours. By comparing the PV parameters listed in Table 2, the decline in R_{sh} for the devices with a longer solution-storage time indicates that more defects or larger leakage current were formed in the photoactive layer which was prepared by the air-exposed solutions.

The optical absorption spectra and the Raman spectra of the P3HT:PCBM films formed by the fresh solution and the air-exposed solutions with a 12-day and 55-day storage time are shown in Fig. 5a and b, respectively. The absorption spectra showed two peaks at 517 and 551 nm and one shoulder at 601 nm in the visible range. These three bands can be attributed to P3HT, while the peak at 334 nm came from PCBM [29,30]. The higher absorption intensity for the films formed by the 12-day and the 55-day solutions were caused by the higher thickness of the film, because when the same spinning speed was used after 12 or 55 days the thicker film was obtained since the volatilization of DCB in the solutions resulted in the higher concentration. The normalized absorption spectra (the inset in Fig. 5a) clearly show the shift of the absorption spectra and the changes of the absorption peaks or shoulders, which can manifest the aggregation and the crystallization states of P3HT and PCBM. For the films formed by the 12- and 55-day stored solutions, the slight blue shift of the absorption spectra in the visible range and the drop of the absorption maximums at 551 and 601 nm were found, which have been attributed to the increased structural defects and the decreased mean conjugated length of P3HT [31,32]. The increase in the short-wave normalized absorption for the 55-day film indicated the formation of the large crystallinity of PCBM, which can hamper the orientation of polymer chain [29,33]. Accordingly, it seems that the degradation of the solar cells by using air-exposed solutions was resulted from physically generated changes in aggregation and crystallization states of P3HT and PCBM.

Raman spectra were used in further study to help identify and analyze molecular structures. In Fig. 5b the P3HT:PCBM films formed by the fresh solution and the air-exposed solutions stored for 12 and 55 days were characterized by Raman spectroscopy in the range of 300–2100 cm^{-1}. The tested samples were prepared by dropping the blend solutions on the glass substrates and obtaining a thick film after the solvent volatilized. The Raman peaks at 1375 and 1438 cm^{-1} correspond to the C–C skeletal stretching and C=C ring stretching vibration, respectively [34–36]. The inset in Fig. 5b shows the same Raman spectra in the range of 1350–1500 cm^{-1}. The Raman frequency of the peak at 1438 cm^{-1} shifted up to 1439 and 1442 cm^{-1} for the films formed by the 12-day and the 55-day solutions, respectively. This up-shift indicated the shortening of the conjugation length along the polymer backbone and a decrease in the crystallinity of P3HT [37,38]. This result was consistent with the blue shift found in the optical absorption spectra of P3HT:PCBM films formed by the air-exposed solutions.

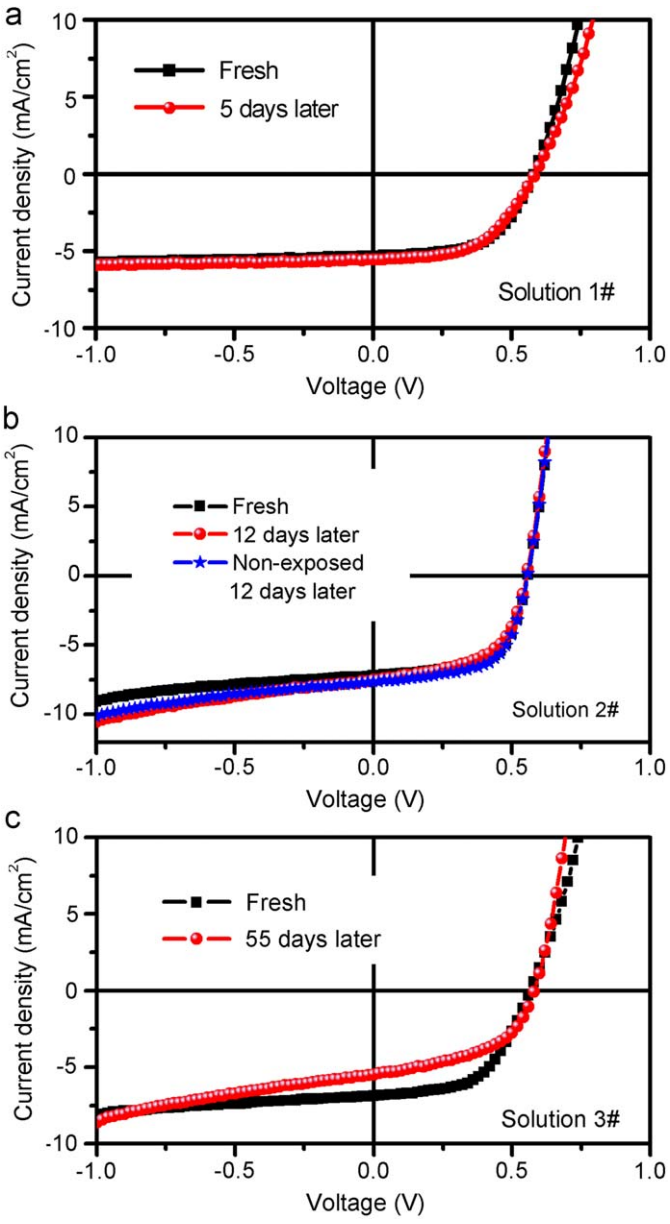

Fig. 4. (a–c) *J–V* characteristics of the samples prepared by the fresh or non-exposed solutions and the air-exposed solutions 1#, 2# and 3#. Solutions 1#, 2# and 3# were stored in the glove box for 5, 12 and 55 days, respectively, after they were exposed to air for a few hours.

Both the optical absorption spectra and the Raman spectra manifested that no new chemical structures were generated and no functional groups disappeared after the blend solutions were exposed to air and stored for a time [39]. Therefore, during the storage time after a few hours' exposure, no chemical oxidation of P3HT or PCBM occurred in the solutions. Besides, the possible explanation that the quenching of PCBM triplet states in the presence of oxygen caused the degradation of polymer solar cell was also unsuitable for this case [40], since all the samples were encapsulated and measured under the almost non-oxygen condition. According to the above spectroscopy analysis, the degradation of polymer solar cells mainly came from the unfavourable morphology of the photoactive film. However, the reason why the air-exposed solutions caused the undesirable aggregation states still need to be researched.

Table 2
Summary of PV parameters of P3HT:PCBM composite devices in Fig. 4a–c.

	Solution 1#		Solution 2#			Solution 3#	
	Fresh	5 days	Fresh	12 days	12 days(non-exposed)	Fresh	55 days
V_{oc} [V]	0.58	0.59	0.56	0.55	0.56	0.57	0.58
J_{sc} [mA/cm^2]	5.34	5.56	7.18	7.50	7.65	6.89	5.47
FF	0.57	0.53	0.63	0.57	0.61	0.55	0.49
η [%]	1.97	1.95	2.71	2.53	2.82	2.14	1.68
R_{sh} (Ω cm^2)	3.16×10^4	4.03×10^4	3.03×10^3	0.95×10^3	1.57×10^3	4.88×10^3	1.14×10^3
R_s (Ωcm^2)	7.89	9.20	3.95	2.83	3.60	7.53	5.08

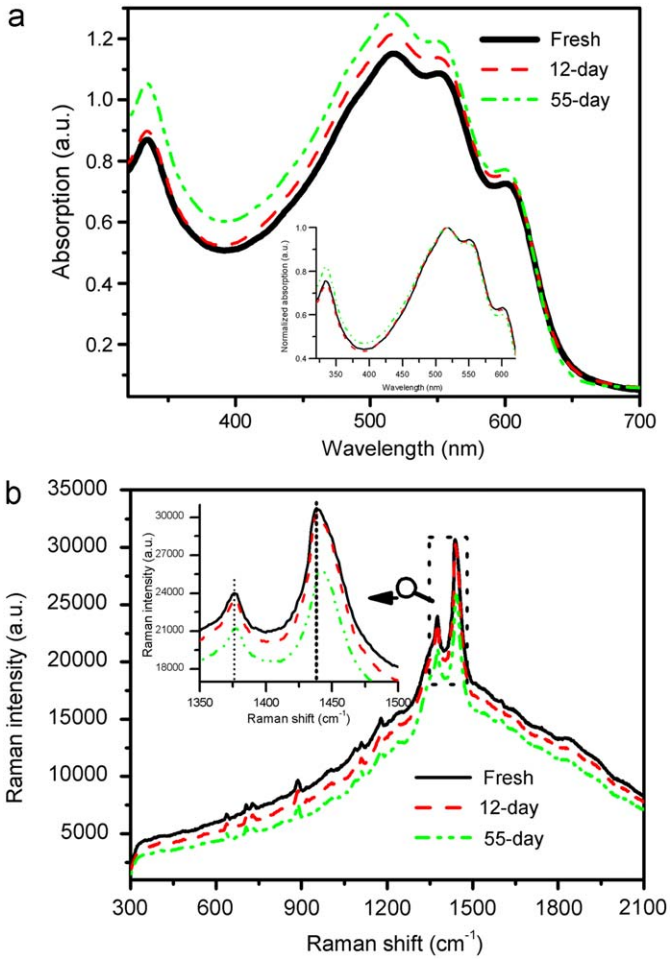

Fig. 5. Optical absorption (a) and Raman spectroscopy (b) of the P3HT:PCBM films formed by the fresh solution and the ever-exposed solutions stored for 12 and 55 days.

4. Conclusions

The proper processing in fabrication can improve the performance of P3HT:PCBM based solar cells. The optimum thickness of spin-coated photoactive layer was determined via experiments and optical modelling. The experimental results clearly correlated with the modelled results. The storage time study showed that exposure of blend solution to air for a few hours will not cause obvious degradation of solar cells within a few days, while the degradation can be enhanced with the increased storage time. Although for each film-processing condition a set of unique parameters need to be exploited, a group of systematical parameters under a given fabrication situation are still valuable for other film-casting methods such as the promising printing technology for plastic solar cells.

Acknowledgements

This work is supported by VTT's Printed Intelligence Strategic Program. The authors thank Martin Kögler for help in Raman spectroscopy analysis.

References

[1] W. Ma, C. Yang, X. Gong, K. Lee, A.J. Heeger, Thermally stable, efficient polymer solar cells with nanoscale control of the interpenetrating network morphology, Adv. Funct. Mater. 15 (2005) 1617–1622.
[2] Y. Kim, S. Cook, S.M. Tuladhar, S.A. Choulis, J. Nelson, J.R. Durrant, D.D.C. Bradley, M. Giles, I. McCulloch, C.-S. Ha, M. Ree, A strong regioregularity effect in self-organizing conjugated polymer films and high-efficiency polythiophene:fullerene solar cells, Nat. Mater. 5 (2006) 197–203.
[3] J. Peet, M.L. Senatore, A.J. Heeger, G.C. Bazan, The role of processing in the fabrication and optimization of plastic solar cell, Adv. Mater. 21 (2009) 15211–15527.
[4] H. Jin, M. Tuomikoski, J. Hiltunen, P. Kopola, A. Maaninen, F. Pino, Polymer–electrode interfacial effect on photovoltaic performances in poly(3-hexylthiophene):phenyl-C61-butyric acid methyl ester based solar cells, J. Phys. Chem. C 113 (2009) 16807–16810.
[5] G. Li, V. Shrotriya, J. Huang, Y. Yao, T. Moriarty, K. Emery, Y. Yang, High-efficiency solution processable polymer photovoltaic cells by self-organization of polymer blends, Nat. Mater. 4 (2005) 864–868.
[6] G. Li, V. Shrotriya, Y. Yao, Yang Yang, Investigation of annealing effects and film thickness dependence of polymer solar cells based on poly(3-hexylthiophene), J. Appl. Phys. 98 (2005) 043704.
[7] W.Y. Huang, C.C. Lee, T.L. Hsieh, The role of conformational transitions on the performance of poly(3-hexylthiophene)/fullerene solar cells, Sol. Energy Mater. Sol. Cells 93 (2009) 382–386.
[8] M. Reyes-Reyes, K. Kim, J. Dewald, R. López-Sandoval, A. Avadhanula, S. Curran, D.L. Carroll, Meso-structure formation for enhanced organic photovoltaic cells, Org. Lett. 7 (2005) 5749–5752.
[9] B. Zimmermann, U. Würfel, M. Niggemann, Longterm stability of efficient inverted P3HT:PCBM solar cells, Sol. Energy Mater. Sol. Cells 93 (2009) 491–496.
[10] J.A. Hauch, P. Schilinsky, S.A. Choulis, R. Childers, M. Biele, C.J. Brabec, Flexible organic P3HT:PCBM bulk-heterojunction modules with more than 1 year outdoor lifetime, Sol. Energy Mater. Sol. Cells 92 (2008) 727–731.
[11] M.O. Reese, A.J. Morfa, M.S. White, N. Kopidakis, S.E. Shaheen, G. Rumbles, D.S. Ginley, Pathways for the degradation of organic photovoltaic P3HT:PCBM based devices, Sol. Energy Mater. Sol. Cells 92 (2008) 746–752.
[12] K. Norrman, S.A. Gevorgyan, F.C. Krebs, Water-induced degradation of polymer solar cells studied by $H_2^{18}O$ labeling, ACS Appl. Mater. Interfaces 1 (2009) 102–112.
[13] M. Jørgensen, K. Norrman, F.C. Krebs, Stability/degradation of polymer solar cells, Sol. Energy Mater. Sol. Cells 92 (2008) 686–714.
[14] R. Tipnis, J. Bernkopf, S. Jia, J. Krieg, S. Li, M. Storch, D. Laird, Large-area organic photovoltaic module—fabrication and performance, Sol. Energy Mater. Sol. Cells 93 (2009) 442–446.
[15] M. Niggemann, B. Zimmermann, J. Haschke, M. Glatthaar, A. Gombert, Organic solar cell modules for specific applications—from energy autonomous systems to large area photovoltaics, Thin Solid Films 516 (2008) 7181–7187.
[16] F.C. Krebs, S.A. Gevorgyan, B. Gholamkhass, S. Holdcroft, C. Schlenker, M.E. Thompson, B.C. Thompson, D. Olson, D.S. Ginley, S.E. Shaheen, H.N. Alshareef, J.W. Murphy, W.J. Youngblood, N.C. Heston, J.R. Reynolds, S. Jia, D. Laird, S.M. Tuladhar, J.G.A. Dane, P. Atienzar, J. Nelson, J.M. Kroon, M.M. Wienk, R.A.J. Janssen, K. Tvingstedt, F. Zhang, M. Andersson, O. Inganäs, M. Lira-Cantu, R. de Bettignies, S. Guillerez, T. Aernouts, D. Cheyns, L. Lutsen,

B. Zimmermann, U. Würfel, M. Niggemann, H.-F. Schleiermacher, P. Liska, M. Grätzel, P. Lianos, E.A. Katz, W. Lohwasser, B. Jannon, A round robin study of flexible large-area roll-to-roll processed polymer solar cell modules, Sol. Energy Mater. Sol. Cells 93 (2009) 1968–1977.
[17] F.C. Krebs, S.A. Gevorgyan, J. Alstrup, A roll-to-roll process to flexible polymer solar cells: model studies, manufacture and operational stability studies, J. Mater. Chem. 19 (2009) 5442–5451.
[18] D.P. Gruber, G. Meinhardt, W. Papousek, Spatial distribution of light absorption in organic photovoltaic devices, Sol. Energy 79 (2005) 697–704.
[19] H. Hoppe, N. Arnold, N.S. Sariciftci, D. Meissner, Modeling the optical absorption within conjugated polymer/fullerene-based bulk-heterojunction organic solar cells, Sol. Energy Mater. Sol. Cells 80 (2003) 105–113.
[20] H. Hoppe, N.S. Sariciftci, D. Meissner, Optical constants of conjugated polymer/fullerene based bulk-heterojunction organic solar cells, Mol. Cryst. Liq. Cryst. 385 (2002) 113–119.
[21] D. Zhu, W. Shen, H. Ye, X. Liu, H. Zhen, Determination of the optical constants of polymer-light emitting diode films from single reflection measurements, J. Phys. D: Appl. Phys. 41 (2008) 235104.
[22] F. Monestier, J.-J. Simon, P. Torchio, L. Escoubas, F. Flory, S. Bailly, R. Bettignies, S. Guillerez, C. Defranoux, Modeling the short-circuit current density of polymer solar cells based on P3HT:PCBM blend, Sol. Energy Mater. Sol. Cells 91 (2007) 405–410.
[23] C.M. Ramsdale, N.C. Greenham, The optical constants of emitter and electrode materials in polymer light-emitting diodes, J. Phys. D: Appl. Phys. 36 (2003) L29–L34.
[24] P.B. Johnson, R.W. Christy, Optical constants of the noble metals, Phys. Rev. B 6 (1972) 4370–4379.
[25] D. Malacara, B.J. Thompson, in: Handbook of Optical Engineering, first ed., Mercel Dekker, New York, 2001.
[26] H. Hoppe, S. Shokhovets, G. Gobsch, Inverse relation between photocurrent and absorption layer thickness in polymer solar cells, Phys. Status Solidi 1 (2007) R40–R42.
[27] F.A. Shirland, The history, design, fabrication and performance of CdS thin film solar cells, Adv. Energy Convers. 6 (1966) 201–222.
[28] S.H. Park, A. Roy, S. Beaupré, S. Cho, N. Coates, J.S. Moon, D. Moses, M. Leclerc, K. Lee, A.J. Heeger, Bulk heterojunction solar cell with internal quantum efficiency approaching 100%, Nat. Photonics 3 (2009) 297–303.
[29] A. Swinnen, I. Haeldermans, P. Vanlaeke, J. D'Haen, J. Poortmans, M. D'Olieslaeger, J.V. Manca, Dual crystallization behaviour of polythiophene/fullerene blends, Eur. Phys. J. Appl. Phys. 36 (2006) 251–256.
[30] V. Shrotriya, J. Ouyang, R.J. Tseng, G. Li, Y. Yang, Absorption spectra modification in poly(3-hexylthiophene): methanofullerene blend thin films, Chem. Phys. Lett. 411 (2005) 138–143.
[31] T.J. Savenije, J.E. Kroeze, X. Yang, J. Loos, The effect of thermal treatment on the morphology and charge carrier dynamics in a polythiophene–fullerene bulk heterojunction, Adv. Funct. Mater. 15 (2005) 1260–12668.
[32] U. Zhokhavets, T. Erb, G. Gobsch, M. Al-Ibrahim, O. Ambacher, Relation between absorption and crystallinity of poly(3-hexylthiophene)/fullerene films for plastic solar cells, Chem. Phys. Lett. 418 (2006) 347–350.
[33] J. Jo, S.-S. Kim, S.-I. Na, B.-K. Yu, D.-Y. Kim, Time-dependent morphology evolution by annealing processes on polymer:fullerene blend solar cells, Adv. Funct. Mater. 19 (2009) 866–874.
[34] Y.-C. Huang, Y.-C. Liao, S.-S. Li, M.-C. Wu, C.-W. Chen, W.-F. Su, Study of the effect of annealing process on the performance of P3HT/PCBM photovoltaic devices using scanning-probe microscopy, Sol. Energy Mater. Sol. Cells 93 (2009) 888–892.
[35] S. Miller, G. Fanchini, Y.-Y. Lin, C. Li, C.-W. Chen, W.-F. Su, M. Chhowalla, Investigation of nanoscale morphological changes in organic photovoltaics during solvent vapor annealing, J. Mater. Chem. 18 (2008) 306–312.
[36] E. Klimov, W. Li, X. Yang, G.G. Hoffmann, J. Loos, Scanning near-field and confocal raman microscopic investigation of P3HT–PCBM systems for solar cell applications, Macromolecules 39 (2006) 4493–4496.
[37] T.-F. Guo, T.-C. Wen, G.L. Pakhomov, X.-G. Chin, S.-H. Liou, P.-H. Yeh, C.-H. Yang, Effects of film treatment on the performance of poly(3-hexylthiophene)/soluble fullerene-based organic solar cells, Thin Solid Films 516 (2008) 3138–3142.
[38] C. Heller, G. Leising, C. Godon, S. Lefrant, W. Fischer, F. Stelzer, Raman excitation profiles of conjugated segments in solution, Phys. Rev. B 51 (1995) 8107–8114.
[39] M. Manceau, A. Rivaton, J.-L. Gardette, S. Guillerez, N. Lemaître, The mechanism of photo- and thermooxidation of poly(3-hexylthiophene) (P3HT) reconsidered, Polym. Degrad. Stabil. 94 (2009) 898–907.
[40] S. Cook, H. Ohkita, Y. Kim, J.J.B. Smith, D.D.C. Bradley, James R. Durrant, A photophysical study of PCBM thin films, Chem. Phys. Lett. 445 (2007) 276–280.